Avalanche Region of IMPATT Diodes

By H. K. GUMMEL and D. L. SCHARFETTER

(Manuscript received August 10, 1966)

The avalanche region of an IMPATT (IMPact ionization Avalanche Transit Time) diode under small signal conditions is characterized by the fraction of the total alternating current that is carried by holes and electrons in their respective drift spaces and by a residual impedance. The current fractions are roughly in phase with the total current below, and nearly 180° out of phase above a resonance frequency that is proportional to the square root of direct current density.

This paper extends the calculations of Gilden and Hines for the current fraction to include phase shifts in the avalanche region so that extended avalanche regions can be considered. Realistic values ($\alpha \neq \beta$ in Si) for the ionization coefficients are used. Results of detailed numerical calculations for the current fractions as a function of frequency and direct current density are presented.

For typical frequencies and current densities, the residual impedance is negligible and hole and electron current fractions are equal. The avalanche region at a given frequency and current density is then characterized by one complex number and the admittance of a diode containing the avalanche region and adjacent drift regions is easily calculated. Plots showing the admittance as a function of frequency and current density for typical structures are given.

It is found that an optimal exponential growth rate of oscillations is obtained when the current density is such that the resonance frequency is about equal to one half the reciprocal transit time through the longest drift region. If the assumption is made that conditions giving the largest small-signal exponential growth rate give the best large-signal performance, an optimum Read-diode design is obtained for which the avalanche region width is a substantial fraction ($\approx \frac{1}{3}$) of the drift region width.

I. INTRODUCTION

This paper considers the avalanche region of IMPATT* diodes,[1,2,3] especially of Read[1]-type diodes in which the avalanche region is localized.

* IMPact ionization Avalanche Transit Time.

Recent theoretical[4] and experimental[5] results for the impedance of Read diodes show considerable structure in the current and frequency dependence. This paper attempts to enhance the understanding of the small-signal negative resistance of IMPATT diodes by isolating the role of the avalanche region. Using the calculated parameters by which the avalanche region is characterized, the admittance for typical IMPATT diodes is calculated and exponential growth rate for oscillations is studied. An application of the results to the design of Read diode oscillators is made.

At a given angular frequency ω and ac terminal current density i_{tot} through the diode, the avalanche region can be characterized by tbree complex numbers: Z_r, F_h, F_e defined below. In Fig. 1, to the right of the avalanche region the small-signal particle current consists of a plane wave of holes. If we assume a constant drift velocity, then the magnitude is constant and the pbase changes linearly with distance. Let A_h be the complex amplitude, extrapolated to a phase reference plane at x_0 in the avalanche region. Then we define the *hole current fraction* F_h

$$F_h = A_h/i_{tot} . \tag{1}$$

Similarly, we define the amplitude of the electron current density, extrapolated to x_0, to be A_e and we define the *electron current fraction* F_e

$$F_e = A_e/i_{tot} . \tag{2}$$

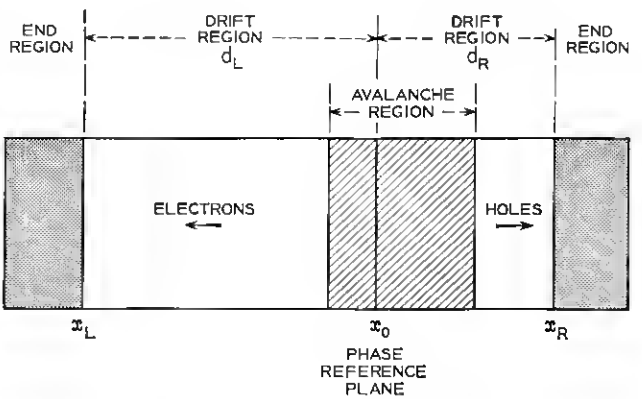

Fig. 1 — Schematic of IMPATT diode.

In the limit as the frequency goes to zero, all the current through the device is particle current and F_h and F_e are of equal magnitude. The phase reference plane is chosen so that at low frequencies F_h and F_e are of equal phase also. The phase reference plane is approximately located at the point where the hole and electron currents are equal.

Assume for a moment that the avalanche region were infinitely thin. From the fact that the total current equals the particle current plus displacement current we find that the ac field per total ac current, to the left of x_0 is

$$\frac{E}{i_{tot}} = \frac{1 - i_e/i_{tot}}{i\omega\varepsilon} = \frac{1 - F_e \exp\left[i\omega(x - x_0)/v_e\right]}{i\omega\varepsilon}, \tag{3}$$

where i_e is the electron current density and v_e the electron velocity. The impedance, Z_{L0} between x_L and x_0 (see Fig. 1) is obtained by integration of (3).

$$Z_{L0} = \frac{1}{i\omega C_L}\left[1 - F_e \frac{1 - \exp\left(-i\omega\tau_L\right)}{i\omega\tau_L}\right], \tag{4}$$

where τ_L is the transit time between x_0 and x_L

$$\tau_L = \frac{x_0 - x_L}{v_e} \tag{5}$$

and C_L is the geometric capacitance per unit area,

$$C_L = \frac{\varepsilon}{x_0 - x_L}. \tag{6}$$

A corresponding expression obtains for Z_{0R}, the impedance between x_0 and x_R.

In deriving (4) it was assumed that the electron current is of the form

$$i_e = F_e \exp\left[i\omega(x - x_0)/v_e\right]. \tag{7}$$

This is true only outside of the avalanche region. The difference between the actual and asymptotic hole and electron current densities gives rise to an additional, *residual* impedance Z_r. The total impedance, exclusive of end-region resistances, is then

$$Z_{tot} = Z_r + Z_{L0} + Z_{0R}. \tag{8}$$

Typically, the residual impedance term is small in comparison to the other terms. Also, for narrow structures and at sufficiently low frequencies such that v/ω is large compared to the width of the avalanche

region, the hole and electron current fractions are equal in value and will be denoted by F without subscript.

In Section II we consider, following Gilden and Hines,[6] the consequences of a simplified model of the avalanche zone, as embodied in Read's (13), (Ref. 1) and derive an expression for F from it

$$F = \frac{1}{1 - \left(\frac{\omega}{\omega_c}\right)^2}. \tag{9}$$

Here the quantity $f_c = \omega_c/2\pi$, which we shall call the *critical frequency*, is real, independent of operating frequency $\omega/2\pi$ and is proportional to the square root of the dc current density.

Section III presents a treatment that is rigorous except for the idealizing assumption that hole and electron velocities are constant and equal in value. Numerical results for several structures are given in Section IV, and it will be shown that for frequencies f and direct current densities of interest F can be represented as

$$F = \frac{(if - B)}{(if - A)(if - \tilde{A})}\left(\frac{A\tilde{A}}{-B}\right), \tag{10}$$

where B is a zero on the real axis and is nearly independent of current density and A and $\tilde{A}$ are complex conjugate poles that traverse a parabolic path in the complex frequency plane as the current density is changed.

In Section V a qualitative description of the change in negative resistance characteristics is given as a transition is made from p-i-n to p-n to "Read" diode. Admittance as function of frequency and current density is shown for two specific structures. Values for the exponential growth rate factor $g(= -1/2Q)$, maximized with respect to frequency, are shown as a function of current density. It is found that an optimal growth rate is obtained when the current density is such that the resonance frequency is about equal to one half the reciprocal transit time through the longest drift region.

In Section VI we explore the consequences of the assumption that best large signal performance is obtained for the same conditions that yield largest small signal growth rate. This assumption in conjunction with a constraint expressing drift-region output limitations leads to Read-diode designs in which the width of the avalanche region is a substantial fraction ($\approx \frac{1}{3}$) of the drift region.

II. SIMPLIFIED MODEL

The current fraction F can be deduced[6] from the simplified theory of Read.[1] His (13) for a thin avalanche region

$$\frac{\tau_1}{2}\frac{dI_0}{dt} = I_0\left(\int \alpha dx - 1\right) + I_s \tag{11}$$

states that the time derivative of the particle current density through the avalanche region, I_0, equals the product of I_0 and a field dependent actor $h(E)$

$$h(E) = \frac{2}{\tau_1}\left(\int \alpha dx - 1\right) \tag{12}$$

if the saturation current I_s can be neglected, as is usually the case. Under dc conditions $h(E) = 0$. If i_p and e represent small signal ac components at frequency ω of particle current density and electric field in the avalanche region, then

$$i\omega i_p = I_0 \frac{\partial h}{\partial E} e. \tag{13}$$

The total alternating current density i_{tot} equals the sum of particle current density and displacement current density,

$$i_{tot} = i_p + i\omega\varepsilon e \tag{14}$$

or, with the definition

$$F = i_p/i_{tot}, \tag{15}$$

$$\frac{e}{i_{tot}} = \frac{1}{i\omega\varepsilon}(1 - F). \tag{16}$$

Division of (13) by i_{tot} and substitution of e from (16) yields

$$F = \frac{1}{1 - j\left(\frac{\omega}{\omega_{crit}}\right)^2} \tag{17}$$

with

$$\omega_{crit} = 2\pi f_{crit} = \sqrt{I_0 \frac{\partial h}{\partial E} \Big/ \varepsilon}. \tag{18}$$

Equations (17) and (18) predict a pole in the impedance or a zero in the admittance at a critical frequency f_{crit} that is proportional to the square root of the current density. Experimental measurements[7] and

numerical calculations[8] have shown that in p-n diodes and p-i-n diodes the admittance goes through a minimum, but not through zero, at frequencies approximately proportional to the square root of current density. This indicates that the simplified theory based on (11) is roughly valid but not accurate in detail. In the next Section a treatment is presented that does not make the assumptions inherent in (11) and that is, therefore, applicable to wide as well as narrow avalanche regions.

III. IMPROVED MODEL

In this section we give a more rigorous treatment of the avalanche zone. The present treatment is facilitated greatly by tbe idealizing assumption that hole and electron velocities are constant and equal in value. If this assumption is not made the problem is still tractable and a method of solution was obtained.[9] However, it is felt that a somewhat idealized treatment with the attendant reduction in complexity and, hopefully, gain in physical insight, is worthwhile. This is especially the case since experimental values for particle velocity vs electric field are available only for prebreakdown fields. Though electron velocities in silicon, the material of present greatest interest, can be extrapolated reasonably well into the breakdown region, considerable uncertainty prevails about hole velocities. However, since in silicon the electrons ionize much more strongly (roughly a factor of 10 more) than holes, it is felt that the results of calculations for the current fractions F are not affected significantly by the choice of hole velocity. Thus, the assumption that the hole velocity equals the electron velocity appears adequate. The value of 10^7 cm/sec is used for the velocity v.

For the ionization coefficients α and β of holes and electrons as function of electric field E the expressions

$$\alpha = 1.8 \times 10^7 \text{ (cm}^{-1}\text{)} \exp\left(-3.2 \times 10^6 \text{ (V/cm)}/E\right)$$

$$\beta = 2.4 \times 10^6 \text{ (cm}^{-1}\text{)} \exp\left(-1.6 \times 10^6 \text{ (V/cm)}/E\right)$$

are used. The numerical values refer to silicon at room temperature and are based on the work of Lee et al.[10]

Let I_h and I_e be the hole and electron current densities. Then the continuity equations state

$$\frac{1}{v}\frac{\partial}{\partial t} I_h = -I_h' + \alpha I_h + \beta I_e \tag{19}$$

$$\frac{1}{v}\frac{\partial}{\partial t} I_e = I_e' + \alpha I_h + \beta I_e \tag{20}$$

where primes denote spatial derivatives. Here we assume that holes move in the $+x$ direction and electrons in the $-x$ direction corresponding to a positive electric field as in an n-p structure. We introduce the total electric current associated with particle motion

$$I_\Sigma = I_e + I_h \tag{21}$$

and the difference in currents

$$I_\Delta = I_e - I_h . \tag{22}$$

Addition of (19) and (20) yields

$$\frac{1}{v}\frac{\partial}{\partial t} I_\Sigma = I_\Delta' + (\beta + \alpha) I_\Sigma + (\beta - \alpha) I_\Delta . \tag{23}$$

From Poisson's equation

$$I_\Delta = -v\varepsilon E' + qvN_D , \tag{24}$$

where E is the electric field and qN_D the net impurity space charge. We shall now again consider small ac quantities at frequency ω, denoted by lower case symbols, superimposed on dc quantities and we denote by i_{tot} the total ac current. From the continuity of total current we obtain

$$i_{\text{tot}} = i_\Sigma + i\omega\varepsilon e. \tag{25}$$

We define

$$k = i\omega/v \tag{26}$$

and normalize the ac electric field to the total alternating current

$$z = \frac{v\varepsilon}{i_{\text{tot}}} e. \tag{27}$$

Then (25) can be written

$$\frac{i_\Sigma}{i_{\text{tot}}} = 1 - kz. \tag{28}$$

We introduce the derivative with respect to field of the last two terms of (23)

$$H = \frac{1}{v\varepsilon}\left[I_\Sigma \frac{\partial}{\partial E}(\beta + \alpha) + I_\Delta \frac{\partial}{\partial E}(\beta - \alpha) \right]. \tag{29}$$

Then the small signal ac version of (23) is

$$-z'' + (\alpha + \beta - k)(1 - kz) - (\beta - \alpha)z' + Hz = 0 \tag{30}$$

or

$$[D^2 - k^2 + (\beta + \alpha)k + (\beta - \alpha)D - H]z = \alpha + B - k, \quad (31)$$

where D is the spatial derivative operator, and where α, β, and H are evaluated for the average, or dc, field as a function of distance.

Equation (31) is a second-order differential equation for the complex quantity z. We postulate that to the left of the avalanche zone all particle current is electron current, i.e.,

$$i_\Sigma = \text{plane wave moving to left} \quad (32)$$

and that to the right of the avalanche zone all particle current is hole current

$$i_\Sigma = \text{plane wave moving to right.} \quad (33)$$

We do *not* specify that the magnitude of the ac electron current on the left equals that of the hole current on the right. Since we differ in this point from previous treatments, some discussion may be warranted.

Holes and electrons are generated in pairs. One might, therefore, be led to conclude that the magnitudes of hole and electron particle currents must be equal. This is true for the dc or average currents but not generally so for the ac currents. Consider that a periodic generation rate $g(x)$ is given. We allow g to be complex to represent the variation in phase with distance. The continuity equations (19) and (20) for the small signal case may be written

$$(k + D)i_h = g \quad (34)$$

$$(k - D)i_e = g. \quad (35)$$

With g considered given, these are first-order differential equations for i_h and i_e. With the boundary conditions (32) and (33) the solutions are

$$i_h(x) = \int_{x_L}^{x} g(s) \exp [-k(x - s)]\, ds \quad (36)$$

$$i_e(x) = \int_{x}^{x_R} g(s) \exp [+k(x - s)]\, ds. \quad (37)$$

Since k is purely imaginary and g is complex, it is seen that $i_h(x_R)$ and $i_e(x_L)$ need not be the same. For narrow structures and at low frequencies, the difference in magnitude is negligible. This, however, is the result of the calculations and not imposed as a constraint.

We specify, then, that outside the avalanche region the particle current consists of a plane wave moving to the left or right.

$$\frac{i_\Sigma}{i_{\text{tot}}} = A_R \exp(-kx) \qquad \text{right} \quad (38)$$

$$\frac{i_\Sigma}{i_{\text{tot}}} = A_L \exp(+kx). \qquad \text{left} \quad (39)$$

The amplitudes A_R and A_L are as yet undetermined. By (28) the electric field outside the avalanche region is

$$z = \frac{1}{k}[1 - A_R \exp(-kx)] \qquad \text{right} \quad (40)$$

$$z = \frac{1}{k}[1 - A_L \exp(+kx)] \qquad \text{left} \quad (41)$$

and we obtain the boundary conditions

$$z' = 1 - kz \qquad \text{right} \quad (42)$$

$$z' = -(1 - kz) \qquad \text{left} \quad (43)$$

in accordance with (22) and (24).

These boundary conditions specify completely the solution of (31). If the solution for z is carried over the entire depletion region, then the integral over z gives the total impedance, exclusive of resistive losses in the end regions. However, in order to isolate the role of the avalanche region and to bring the impedance into the form (8) we proceed as follows: If a solution for z has been obtained at some sufficiently low frequency, then the magnitudes of A_R and A_L in (38) and (39) are equal. A value x_0 exists at which the right hand side of (38) equals the right hand side of (39); i.e., at which the asymptotic particle currents, extrapolated into the avalanche zone, are equal in phase as well as magnitude. We call x_0 the phase reference point and define the extrapolated particle currents at this point as the current fractions F_e and F_h ;

$$F_h = A_R \exp(-kx_0) \qquad (44)$$

$$F_e = A_L \exp(+kx_0). \qquad (45)$$

We define the asymptotic particle current i_a ,

$$i_a/i_{\text{tot}} = \begin{cases} F_h \exp[-k(x - x_0)] & x \geqq x_0 \\ F_e \exp[+k(x - x_0)] & x < x_0 \end{cases} \qquad (46)$$

and the residual particle current i_r as the difference between the actual particle current $i_{\text{tot}}(1 - kz)$ and the asymptotic particle current

$$\frac{i_r}{i_{\text{tot}}} = 1 - kz - \frac{i_a}{i_{\text{tot}}}. \tag{47}$$

Note that by construction i_r vanishes outside the avalanche zone and is thus independent of the dimensions of the drift zones, as are F_e and F_h. We can now solve (47) for z,

$$z = \frac{1}{k}\left[1 - \frac{i_r}{i_{\text{tot}}} - \begin{cases} F_h \exp\left[-k(x - x_0)\right] & x \geqq x_0 \\ F_e \exp\left[+k(x - x_0)\right] & x < x_0 . \end{cases}\right] \tag{48}$$

The integral of z, multiplied by $1/v\varepsilon = k/(i\omega\varepsilon)$ is the total impedance

$$Z = Z_r + \frac{x_0 - x_L}{i\omega\varepsilon}\left[1 - F_e \frac{-\exp(i\omega\tau_L)}{i\omega\tau_L}\right] + \frac{x_R - x_0}{i\omega\varepsilon}\left[1 - F_h \frac{1 - \exp(i\omega\tau_R)}{i\omega\tau_R}\right] \tag{49}$$

$$= Z_r + Z_{L0} + Z_{0R}, \tag{50}$$

with

$$Z_r = -\frac{1}{i\omega\varepsilon}\int \frac{i_r}{i_{\text{tot}}}\, dx. \tag{51}$$

We shall use the symbol F without subscript to refer to either F_e or F_h if their difference is negligible or the distinction unimportant.

IV. NUMERICAL RESULTS

This section contains numerical results for the following structures in silicon:

- *D3* error function complement p-diffusion from a surface concentration of 10^{20} cm^{-3} into a 3×10^{16} cm^{-3} n-type substrate with a junction depth of 3 microns.
- D12 similar to D3, but with a 12-micron junction depth.
- L22 a linearly graded junction with a concentration gradient of 10^{22} impurities/cm^4.
- C0.1 Constant field avalanche zone (field = 5.71×10^5 volts/cm) of 0.1-micron width, surrounded by regions of sufficiently low field that negligible avalanching takes place there.
- C1 Similar to C0.1, but with 1-micron width; field = 3.57×10^5 volts/cm.
- C5 Similar to C0.1, but with 5-micron width; field = 2.79×10^5 volts/cm.

C10 Similar to C0.1, but with 10-micron width; field = 2.52×10^5 volts/cm.

For each desired direct current density I_Σ, self-consistent values of dc electric field E, difference current density I_Δ, ionization coefficients α and β, and derivative quantity H, (29), were computed as described in Appendix A. Using these quantities, the differential equation (31), subject to boundary conditions (42) and (43), was solved numerically for k-values corresponding to frequencies of interest.

Figs. 2 and 3 show the results for the quantity $1 - 1/F =$ (−displacement current/particle current) for direct current densities of 100 and 1000 amps/cm^2. According to the simplified model of Section II, $1 - 1/F$ should have a real part varying as the square of frequency and a vanishing imaginary part. As Figs. 2 and 3 show, the square law is obeyed quite well at low frequencies and current densities. Only for the wide structures and/or at high frequencies and current densities does F deviate from the square law and do F_e and F_h deviate from each other appreciably. The frequency f_{crit} at which $(1 - 1/F)_{real}$ is unity

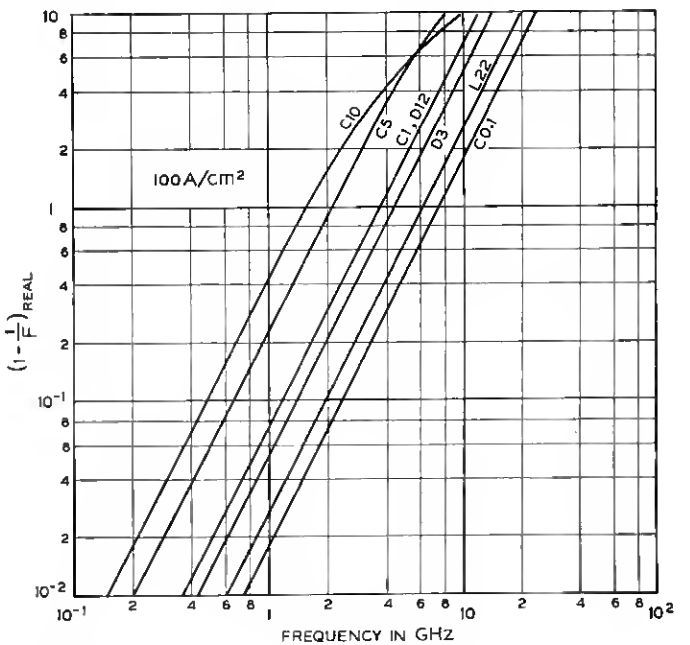

Fig. 2 — Real part of 1 − 1/F as function of frequency for various structures. Current density 100 amps/cm^2.

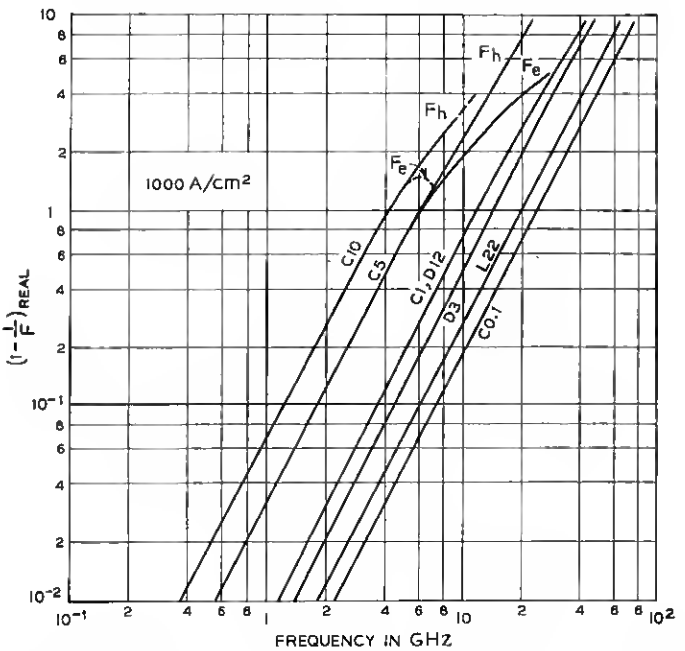

Fig. 3 — Real part of $1 - 1/F$ as function of frequency for various structures. Current density 1000 amps/cm².

is in good agreement with values obtained from the simple theory of Section II.

The absolute value of the imaginary part of $1 - 1/F$ at a current density of 100 amp/cm² is plotted in Fig. 4 as a function of frequency f for the various structures. The current dependence of the diffused diode D3 is shown in Fig. 5; that for the other structures is similar. The vertical line on each curve to the right of the maximum indicates the frequency at which the real part goes to zero. At frequencies 15 to 25 percent higher, $(1 - 1/F)_{imag}$ goes through zero, being positive for lower and negative for higher frequencies. Asymptotically, at low frequencies $(1 - 1/F)_{imag}$ is proportional to $+f$ and at higher frequencies to $-f^3$. The similarity of the curves is striking and suggests that a fit with a few parameters ought to be possible. The most meaningful expansion, and one working well here, is to consider F as an analytical function of a complex frequency variable and to expand it in terms of the poles and zeroes nearest the frequency domain of interest. At current densities of interest and for frequencies f from zero to a few times

f_{crit}, the numerical results can be represented well by two poles and a zero;

$$F = \frac{(if - B)}{(if - A)(if - \tilde{A})} \cdot \frac{A\tilde{A}}{-B}, \tag{52}$$

where $\sim$ denotes the complex conjugate. A is the complex resonance frequency

$$A = f_a + if_r . \tag{53}$$

We denote

$$B = -f_c .$$

We utilize the following inequalities which hold for current densities of interest:

$$f_a \ll f_r \tag{54}$$

$$f_r \ll f_c \tag{55}$$

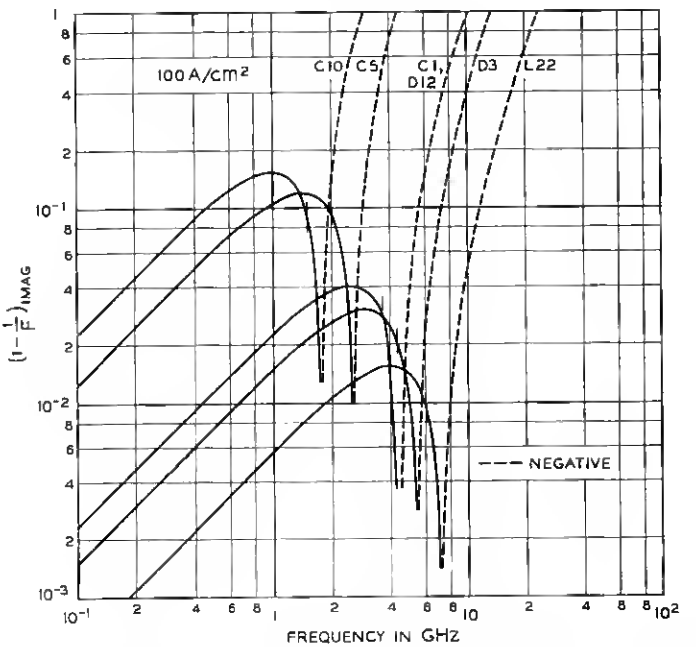

Fig. 4 — Imaginary part of 1 − 1/F as function of frequency for various structures. Current density 100 amps/cm². The vertical bars indicate f_{crit}.

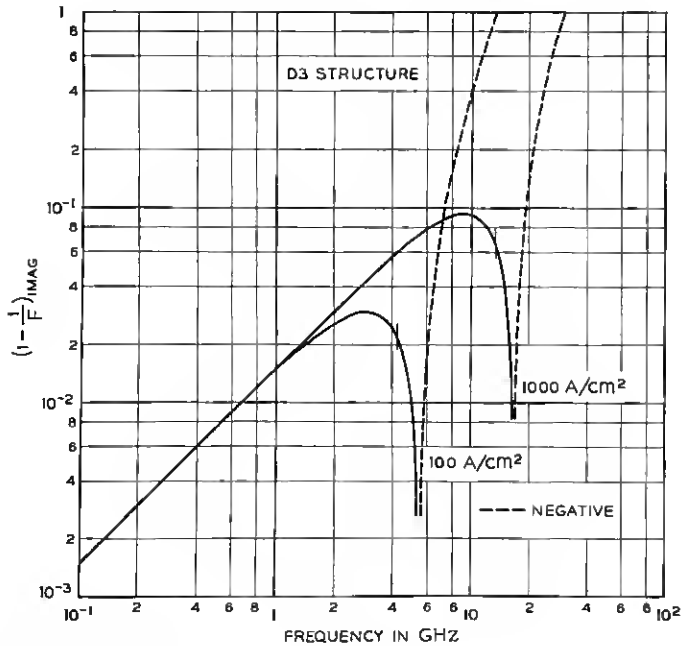

Fig. 5 — Imaginary part of $1 - 1/F$ as a function of current density for diode D3 at 100 and 1000 amps/cm².

and we consider frequencies small compared to f_c. Then the reciprocal of (52) can be written

$$\frac{1}{F} = 1 - \frac{f^2}{f_r^2} - if\left(\frac{1}{f_c} + \frac{2f_a}{f_r^2} - \frac{f^2}{f_c f_r^2}\right). \tag{56}$$

Equation (56) has the frequency dependence embodied in Figs. 2 through 5, i.e., the real part of $1 - 1/F$ changes as frequency squared and the imaginary part is the difference of a linear and cubic term in frequency. The low-frequency asymptote of the imaginary part is

$$(1 - 1/F)_{\text{imag}} = f/f_s\,, \tag{57}$$

with

$$f_s = \frac{f_c}{1 + 2f_a f_c/f_r^2}\,. \tag{58}$$

The frequency, f_{crit}, at which the real part of $1/F$ vanishes equals f_r:

$$f_{crit} = f_r \tag{59}$$

and the frequency f_i at which the imaginary part of $1/F$ vanishes is

$$f_i = \sqrt{f_r^2 + 2f_a f_c}\,. \tag{60}$$

Now let us consider the dependence of F on the direct current density I. Three relations hold approximately for the curves of Figs. 2 through 5.

The critical frequency f_{crit} is proportional to the square root of direct current density. (61)

The low-frequency, linear asymptote of $(1 - 1/F)_{imag}$ is independent of current density. (62)

The ratio of the frequencies f_{crit} and f_i at which the real and imaginary parts of $1/F$ cross zero is independent of current density. (63)

We show now that these relations lead to the following current density dependences:

$$f_a \propto I \tag{64}$$

$$f_r \propto \sqrt{I} \tag{65}$$

$$f_c \text{ independent of } I. \tag{66}$$

Equation (65) follows directly from (59) and (61). Taking the ratio of (60) and (59) and using (63) we find that

$$f_a f_c / f_r^2 \text{ is independent of } I. \tag{67}$$

Use of (62), (57), (58), and (67) yields (66). Finally, from (65), (66), and (67) we obtain (64). Thus, as long as the inequalities (54) and (55) and relations (61) through (63) hold, the current density dependence of F can be expressed as follows (see Fig. 6): *With increasing current density the poles A and $\tilde{A}$ of F move through parabolas, starting at the origin, while the zero at $-f_c$ is independent of current density.* Where F_e and F_h deviate from each other, the representation (52) is still usable. The poles A and $\tilde{A}$ are the same, but F_e and F_h have separate zeros at $-f_{ce}$ and $-f_{ch}$.

The above discussion shows how the poles and zero can be obtained from calculated results of F as a function of frequency and current density. In Appendix B a more direct way of obtaining the poles as solutions of an eigen-value problem is presented. The results are shown in Fig. 6, where the poles are plotted in the complex frequency plane with current density varying along the curves. The zeroes are listed in the insert. Only positive imaginary values are shown. Symmetry exists about the

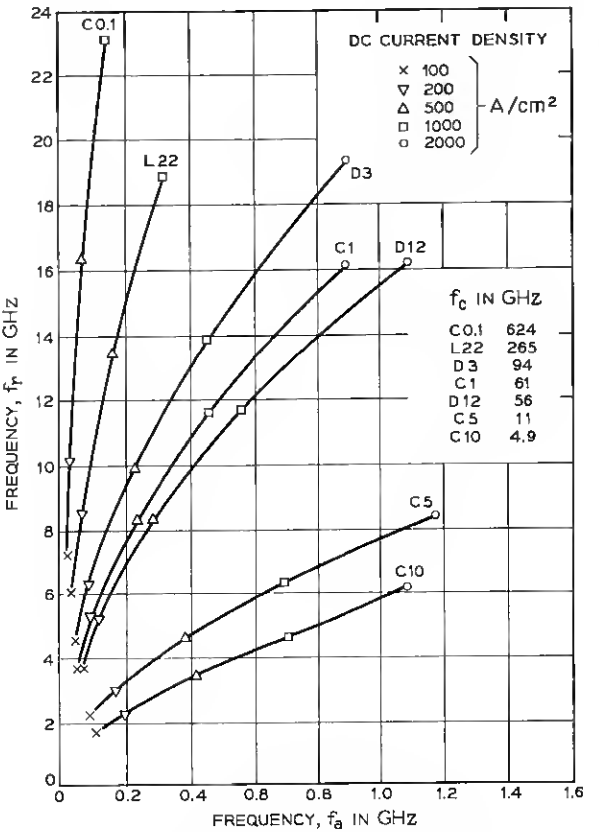

Fig. 6 — Locus of poles of F as function of current density in the complex frequency plane. Note unequal scales of real and imaginary axes.

real axis. Note that the scales of real and imaginary axes differ hy a factor of 10.

V. NEGATIVE RESISTANCE AND MAXIMUM GROWTH FACTOR

In this section, we consider the interaction of the avalanche and drift regions in causing negative resistance. The most important aspect of the current fraction F is the rapid change of phase, with respect to total current, from near zero below, to more than 180° above, the resonance frequency. This behavior follows from (52) and is illustrated for structure D3 in Fig. 7 where the phase φ_F of F is shown for current densities of 100 and 1000 A/cm^2. At the higher current density the transition is

more gradual. Likewise, for wider structures the transition is more gradual than for narrower structures.

Let us consider a diode in which the hole drift region is negligible and for which the residual impedance Z_r is negligible so that the dominant term in the impedance is

$$Z_{L0} = \frac{1}{i\omega C_L}\left[1 - F\frac{1 - \exp(-i\omega\tau_L)}{i\omega\tau_L}\right]. \tag{68}$$

We want to explore under what conditions the small signal impedance has a negative real part. This will occur when the quantity

$$F\frac{1 - \exp(-i\omega\tau_L)}{i\omega\tau_L} \equiv FG \tag{69}$$

has a phase angle between 0 and 180°. φ_G, the negative of the phase of G, is plotted in Fig. 8 as a function of frequency. We define as drift frequency, f_{drift}, the frequency at which the phase φ_G is 90°,

$$f_{\text{drift}} = \frac{v}{2(x_0 - x_L)} = \frac{1}{2\tau_L}. \tag{70}$$

The singularity at twice the drift frequency occurs where G goes to zero and the phase is indeterminate. If the operating frequency is below $1/\tau_L$ we refer to the diode as operating in the π mode. The mode-

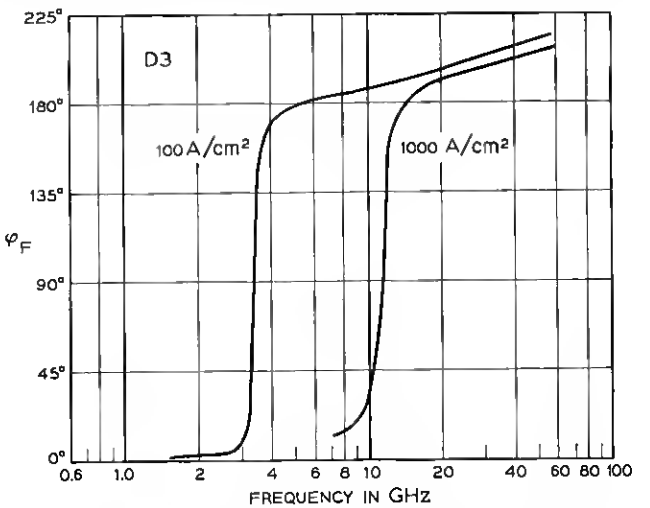

Fig. 7 — Phase of F for diode D3 at 100 and 1000 amps/cm².

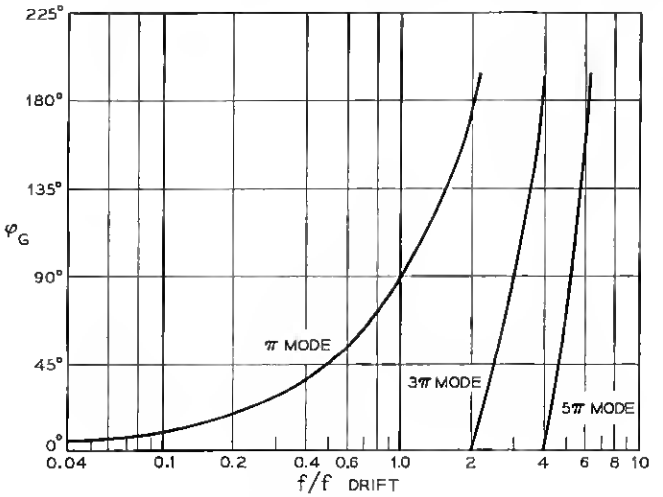

Fig. 8 — Negative of drift delay phase.

designation for higher frequencies is given in Fig. 8. The condition on the phases for negative resistance can now be stated

$$0 < \varphi_F - \varphi_G < 180° \tag{71}$$

and can easily be visualized if Figs. 7 and 8 are combined. This has been done in Fig. 9 where a drift frequency of 60 GHz appropriate for the depletion layer of diode D3 has been used. Starting with the 100 A/cm^2 curve for φ_F, we see that negative resistance prevails over a wide frequency range, as indicated by the shaded region. Near $f = 2f_{\text{drift}}$ the magnitude of G is small, hence the negative resistance contribution of FG is small and is likely to be outweighed by parasitic end resistance. At frequencies beyond $2f_{\text{drift}}$ negative resistance occurs in higher-order modes. At frequencies much higher than f_{crit} the phase φ_F depends on frequency in a complicated way and the present calculations lose accuracy. As the current density is increased, the φ_F curve moves to the right with some softening of the transition. The lowest frequency at which negative resistance sets in increases also, but a wide range of negative resistance continues to exist. The behavior thus far described is typical of a single-diffused p-n junction diode.

Next, consider a typical "Read" structure, i.e., one in which the drift space is much wider than the avalanche region. We consider the same avalanche zone as before but let the drift space be, say 8 microns

with a drift frequency of 6.25 GHz, as shown in Fig. 10. We now see that the frequency range for negative resistance in the π mode is much narrower; at 1000 A/cm^2 there is no π-mode negative resistance for this structure.

Now let us consider structures with narrow drift regions. The extreme case for which the drift regions coincide with the avalanche region is represented by p-i-n diodes.[8] All three terms in (8) contribute, but the conclusions reached from a study of Z_{L0} alone are qualitatively correct. Negative resistance is obtained for a wide range of frequencies. For a consideration of the low-frequency behavior we expand F to first order in f

$$F \approx 1 + i\frac{f}{f_s} \tag{72}$$

(cf. (57) and (58). With

$$G \approx 1 - \frac{i\omega\tau_L}{2} = 1 - i\frac{\pi f}{2f_{\text{drift}}} \tag{73}$$

(68) yields

$$R_{L0} = \frac{1}{4f_{\text{drift}}\, C_L}\left(1 - \frac{2f_{\text{drift}}}{\pi f_s}\right). \tag{74}$$

Thus, if

$$f_{\text{drift}} < \frac{\pi}{2} f_s\,, \tag{75}$$

negative resistance prevails from π mode frequencies down to dc. The case of the uniform-field avalanching plasma has been discussed by Misawa.[8]

For an interpretation of the frequency f_s, consider the change in electric field δE, per change in total current in the limit as the frequency goes to zero, as shown in Fig. 11, for diode D3 at 100 A/cm^2. The space charge associated with the additional current causes δE to be roughly hyperbolically shaped with the apex at the point where hole and electron currents are equal. The placement of the δE curve with respect to zero is such that reduction of ionization in the center where δE is negative is compensated by an increase in the adjacent regions. Outside the avalanche zone δE changes linearly. At points A and B, separated by distance d_{AB} the asymptotes to δE outside the avalanche zone cross zero. From a consideration of (28) through (32) it can be seen that $1/f_s$ is half the transit time between points A and B,

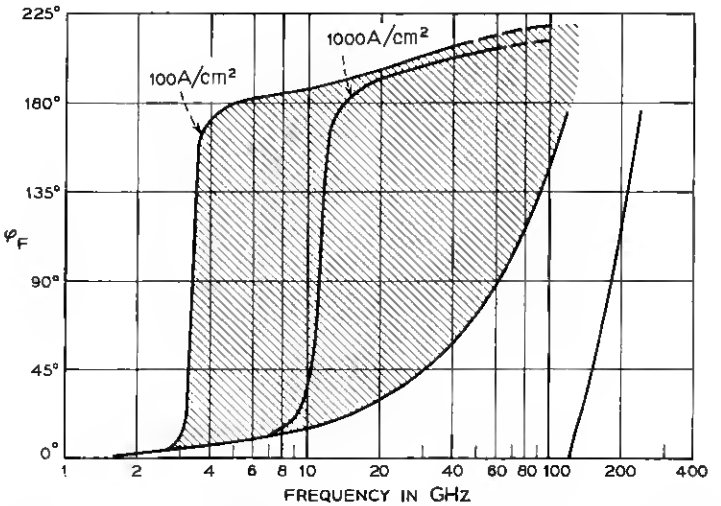

Fig. 9 — Superposition of Figs. 8 and 9 appropriate for p-n junction case.

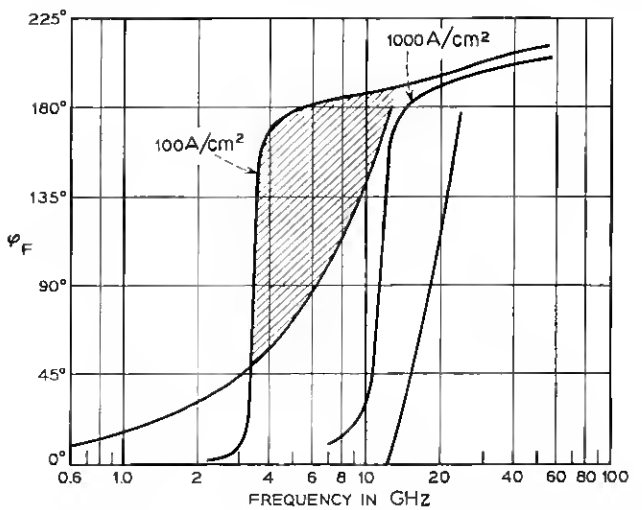

Fig. 10 — Superposition of Figs. 8 and 9 appropriate for "Read" diode case.

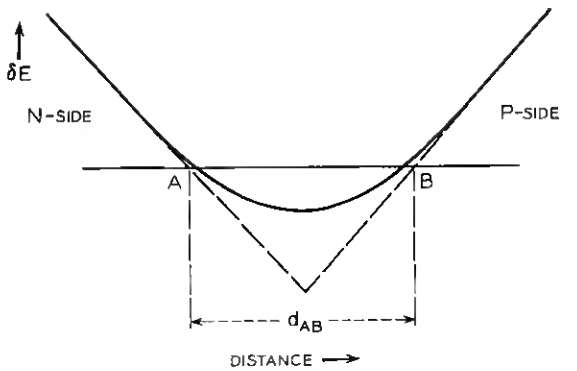

Fig. 11 — Incremental field at low frequencies for p-n diode.

$$f_s = \frac{d_{AB}}{2v}. \tag{76}$$

If the avalanche zone is narrow compared to the drift region the integral over δE is positive and so is the dc incremental resistance.

For a p-i-n diode (C1 at 100 A/cm^2) the incremental field δE is as shown in Fig. 12. The asymmetry results from the inequality of hole and electron ionization coefficients. It is seen by inspection that the integral over δE is negative and also that the transit time between A and B is less than $\pi/2$ times the transit time through the depletion layer (this is the condition corresponding to (75) when both left and right drift regions are considered), hence the resistance is negative. It is to be noted, however, that if equal hole and ionization rates had been used in this calculation, zero incremental dc resistance would have been obtained.

Up to this point we have considered the phase conditions for the occurrence of negative resistance. Now let us consider the actual resistance or, more conveniently, the admittance Y. Fig. 13 shows plots of the imaginary vs real part of Y, with frequency varying along each curve, for diode D3, area = 10^{-4} cm^2, at various current densities. Fig. 14 shows a corresponding plot for a Read structure R1 consisting of avalanche region C1 (1 micron wide, constant field) and an adjacent electron drift space 9 microns wide. The diode area is also taken as 10^{-4} cm^2. The admittances in Figs. 13 and 14 are the reciprocal total impedance, but differ insignificantly from what would have been obtained with neglect of the residual impedance.

Now let us consider the quality factor Q or the related *growth factor* g,

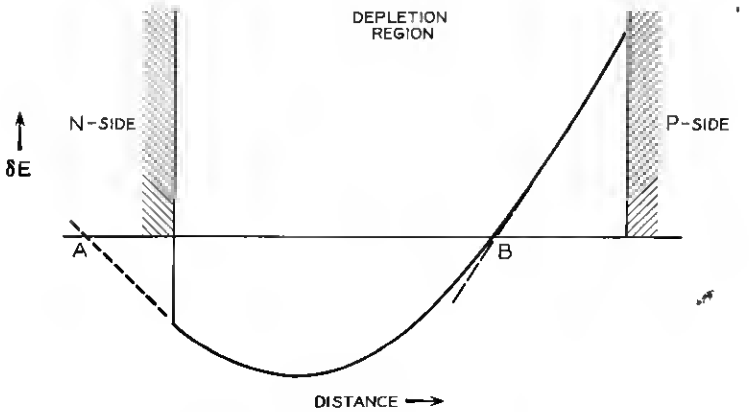

Fig. 12 — Incremental field at low frequencies for p-i-n diode.

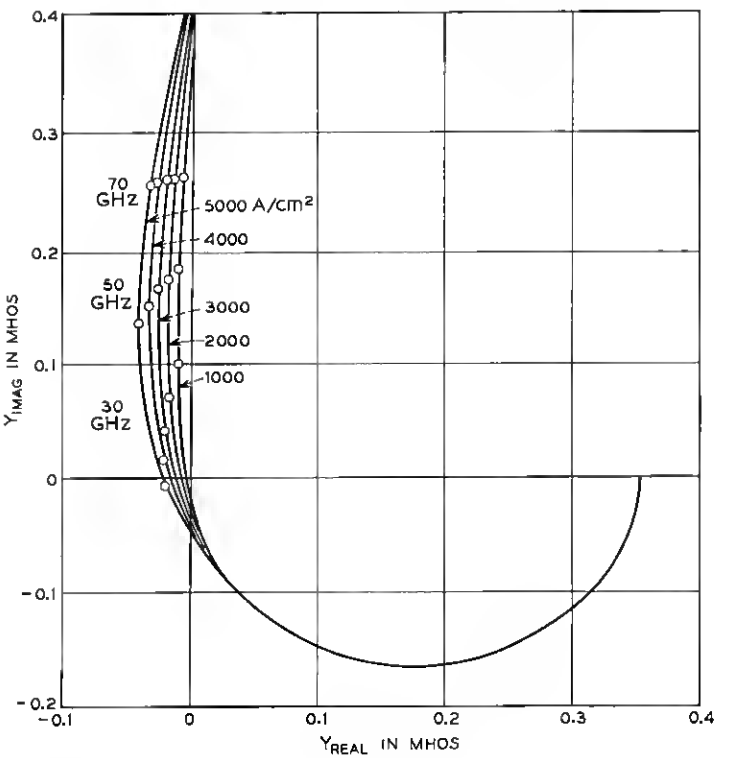

Fig. 13 — Admittance of diode D3. Selected frequencies, in GHz, are marked off on each curve.

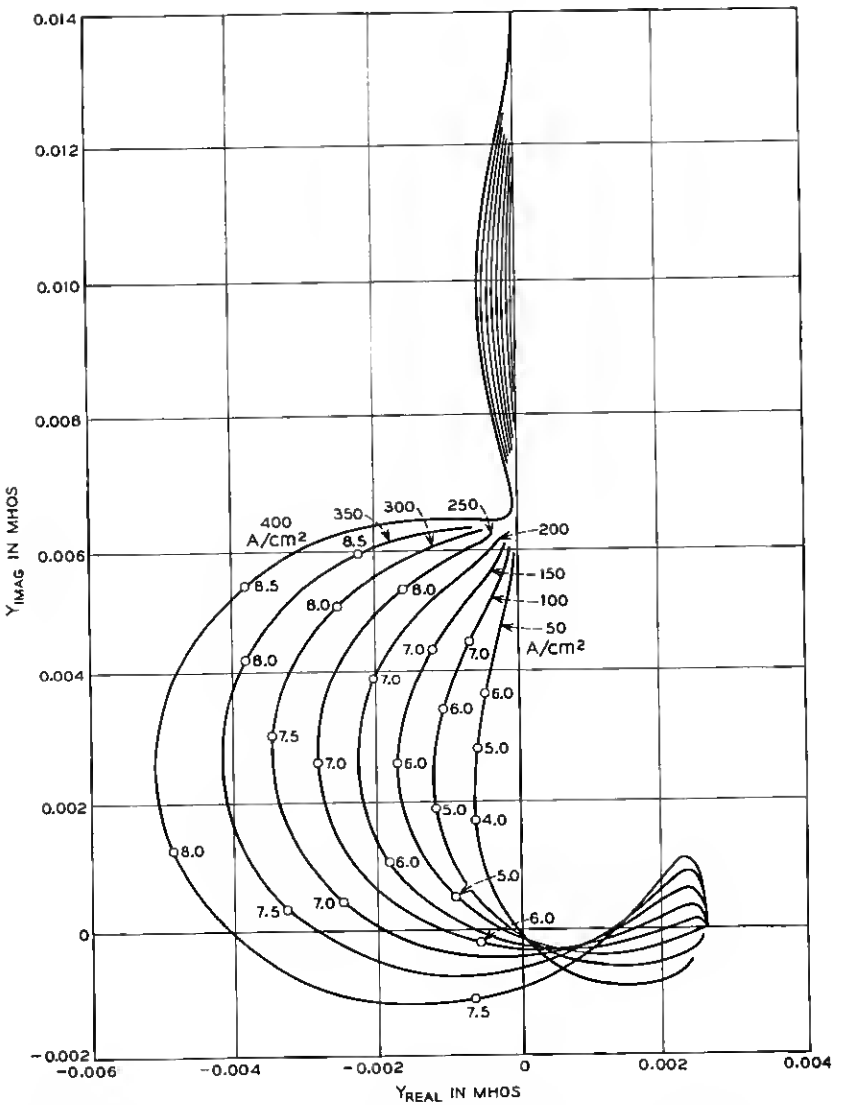

Fig. 14 — Admittance of Read diode R1. Selected frequencies, in GHz, are marked off on each curve.

$$g = -\frac{1}{2Q} \tag{77}$$

which has the following meaning: If a diode having negative resistance is imbedded in a lossless circuit in which it oscillates at frequency $f = \omega/2\pi$, then the absolute values of voltage and current amplitudes vary with time as exp $(g\omega t)$. It is convenient to introduce the complex frequency variable s

$$s = (g + i)f. \tag{78}$$

From (4), (52), and (53) it can be inferred that under open-circuit conditions the diode will oscillate at a value

$$s = A = f_a + if_r$$

and, therefore, the open-circuit growth factor is

$$g_{\text{open}} = f_a/f_r .$$

According to the current-dependence of Fig. 6, g_{open} is proportional to the square root of the current density. Note that under open-circuit conditions g depends on the avalanche structure only and is independent of the drift regions. This is not the case under more general circuit conditions.

If the admittance Y is an analytic function of frequency, as is physically reasonable and as we shall assume to be the case here, then the admittance is defined also for complex frequencies. The largest growth rate $g(f)$ for reactive circuit imbedding at a given frequency f is that g for which

$$Y[(g + i)f] + \frac{1}{2\pi(g + i)fL} = 0 \tag{79}$$

if Y is capacitive; or

$$Y[(g + i)f] + 2\pi(g + i)fC = 0 \tag{80}$$

if Y is inductive. Here L or C are chosen so as to resonate the imaginary part of Y. The quantity g thus obtained is related to the quality factor Q, as conventionally defined, by (77). So far, g is defined at a given frequency f and current density. We define as $g_{\max}$ the maximum of g (or maxima, where relative maxima exist) with respect to frequency at a given current density. Finally, we define as g_{opt} the maximum of $g_{\max}$ with respect to current density. We define by $f_{\max}$ the frequency (ies) at which $g_{\max}$ occurs. Figs. 15 and 16 show $g_{\max}$ and $f_{\max}$ as a function

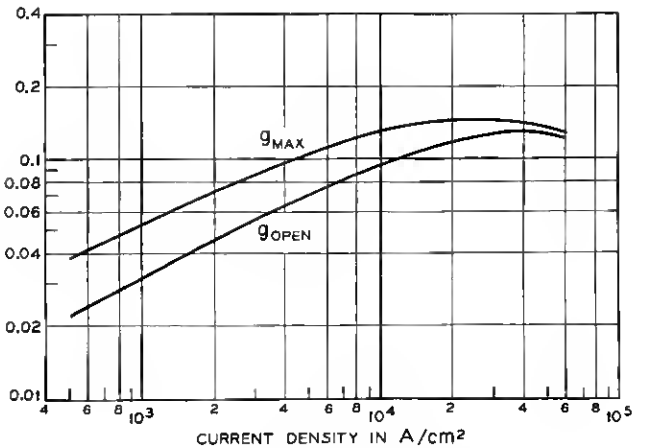

Fig. 15 — Maximum growth rate and open-circuit growth rate of diode D3.

of current density for diode D3 and Figs. 17 and 18 for diode R1. Also shown for comparison are f_r and g_{open}. Included in Figs. 16 and 18 are horizontal lines marked f_{drift} representing the drift frequency of the longest (= electron) drift region. An important result contained in Figs. 15 to 18 is that g_{opt} is obtained for current densities at which the resonance frequency f_r is about equal to the drift frequency and that

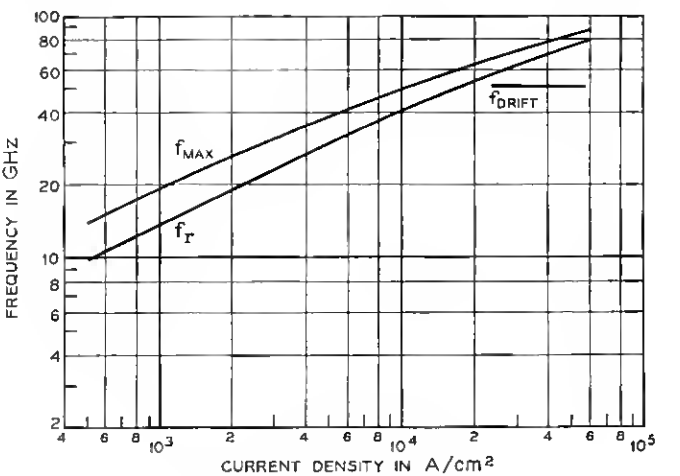

Fig. 16 — Frequency at which g_{max} occurs and f_r for diode D3.

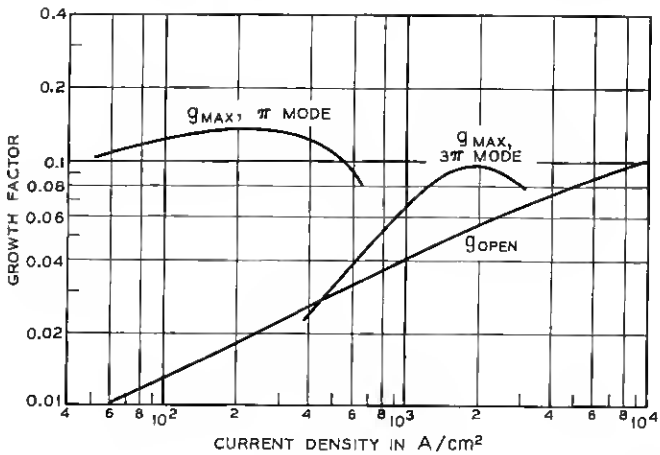

Fig. 17 — Maximum growth rate and open circuit growth rate for Read diode R1.

f_{max} at this current density is some 20 to 30 percent above f_r. For the diffused diode D3 the drift frequency is higb ($\approx$ 60 GHz) and tberefore, g_{opt} is obtained at a high current density, 3×10^4 amps/cm^2. This current density is so high that a substantial widening of the avalanche region, with respect to its low-current-density configuration, bas taken place. As a consequence, f_c now is no longer independent of current density, but rather decreases with current density. Deviations from the low-current-density relations are also seen in the breakaway from tbe line of slope $\frac{1}{2}$ for g_{open} in Fig. 15.

For the Read diode R1 the largest g_{opt}, occurring in the π mode, is obtained at 200 amps/cm^2. The values of g_{max} in the $n\pi$ mode fall off rapidly as the frequency approacbes $(n + 1)f_{drift}$. For a Read-type structure, i.e., one having a substantial drift space in which negligible avalanche multiplication takes place, g_{opt} is near 0.13 and is only weakly dependent of the detailed structure of tbe avalanche region. On the other hand, for diodes in which the avalancbe region occupies all of, or a substantial fraction of, the depletion region g_{opt} is closely related to the value of g_{open} and is larger than 0.13, as is the case for D3.

VI. LARGE SIGNAL DESIGN CONSIDERATIONS FOR READ DIODES

In Section V we obtained the result that the optimum growth rate under small-signal conditions occurs when $f_{drift} \approx f_r$. This condition

provides a relation between current density, drift region width and avalanche region width (via f_r). It is plausible to assume that the same relation should be approximately satisfied for best large-signal performance. Preliminary large-signal results* have shown that a direct correspondence between the large-signal and small-signal properties does not exist and that, for example, large-signal self-sustained oscillation can be obtained for frequency-current-density combinations for which the small-signal resistance is positive. Nevertheless, as a point of departure for a large-signal design we choose a structure in which avalanche region, drift region, and current density are so related that g_{opt} is obtained at

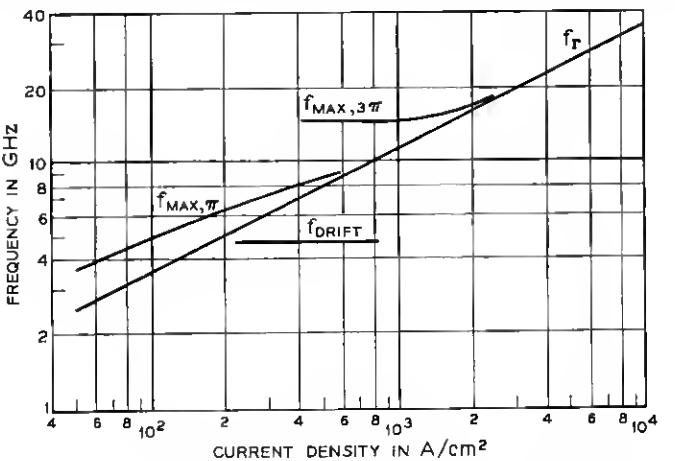

Fig. 18 — Frequency at which g_{max} occurs and f_r for diode R1.

the desired frequeney under small signal conditions. This provides one constraint.

Resonance frequency f_r as a function of current density for the various structures is shown in Fig. 19. Suppose a 5-GHz operating frequeney is wanted. We would need a resonance frequency about 25 percent lower or 4 GHz. Thus, structure C1 at 120 amps/cm², or C5 at 400 amps/cm², etc. could be used. The drift region would be 12.5 microns wide.

Another constraint between average current density and frequency is imposed by the output limitations of the drift space. The following discussion applies to Read diodes having a constant-field drift region only. As shown by Read,[1] under large-signal conditions the carrier current through the drift region is carried in the form of charge pulses. If

* D. L. Scharfetter and H. K. Gummel, work in progress.

f is the frequency of operation and I_{DC} the average current density, then the charge per pulse is

$$Q = \frac{I_{DC}}{f}. \tag{81}$$

This pulse causes a change in electric field of

$$\Delta E = \frac{I_{DC}}{(\varepsilon f)}. \tag{82}$$

Let E_{drift} be the field in the drift region at the onset of breakdown; we shall use a value of 1.5×10^5 V/cm which is reasonable for silicon. ΔE must not be larger than approximately $\frac{1}{2} E_{\text{drift}}$. The factor of $\frac{1}{2}$ takes into account that in the desired mode of operation the terminal voltage reaches its minimum while the charge moves through the drift region and that therefore an additional lowering of the drift field below E_{drift} occurs. Thus, we have the condition

$$I_{DC} < \tfrac{1}{2}\varepsilon E_{\text{drift}} f. \tag{83}$$

This constraint is shown in Fig. 19 by the line of slope 1. Only the region to the upper left is allowed. For a diode to have a largo power capability the highest feasible current density should be used. Thus, a design cor-

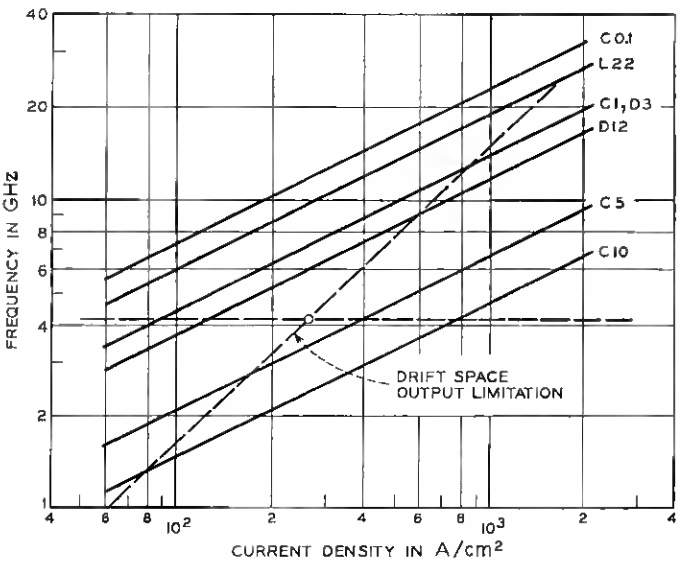

Fig. 19 — Illustration of Read diode design considerations.

responding to the circle appears most promising. The diode would operate at a current density of 300 amps/cm^2 and have an avalanche region 4 microns wide. Note that the avalanche region width would be about $\frac{1}{3}$ of the drift region width. This is in contrast to Read's proposal that the avalanche region should be very narrow in comparison to the drift region. However, the design suggested here is based on a combination of small-signal dynamics and large-signal output limitations and may have to be modified when large-signal results become available.

APPENDIX A

This appendix describes the steps by which self-consistent dc solutions for electric field E and difference current density I_Δ are obtained for a given terminal current density I_Σ. The electric field is the sum of a component $E_D(x)$, related to the space charge of the impurities and a component

$$E_C(x) = (\epsilon v/I_\Sigma)z(x),$$

where $z' = I_\Delta/I_\Sigma$, related to the space charge of the mobile carriers.

(*i*) Select a point x_1 in the avalanche region and assign a trial value E_1 for the electric field at this point. Conveniently, x_1 may be the location of the metallurgical junction, but the choice is not critical.

(*ii*) Choose a trial function for the difference current I_Δ. A convenient, though crude, choice is

$$I_\Delta = I_\Sigma, \qquad x \leqq x_1 \tag{84}$$

$$I_\Delta = -I_\Sigma, \qquad x > x_1. \tag{85}$$

(*iii*) Compute the electric field E

$$E(x) = E_1 + \frac{1}{\epsilon}\int_{x_1}^{x}\left[\frac{I_\Delta(s)}{v} + qN_D(s)\right]ds. \tag{86}$$

Extend the integral up to boundary points x_L and x_R to the left and right of x_1, i.e., to points where the field reaches the value required to carry the current through the not swept-out semiconductor region:

$$E(x_L) = I_\Sigma/[\mu_n \mid N_D(x_L) \mid] \tag{87}$$

$$E(x_R) = I_\Sigma/[\mu_p \mid N_D(x_R) \mid]. \tag{88}$$

Define

$$E_D(x) = E_1 + \frac{q}{\epsilon}\int_{x_1}^{x} N_D(s)\,ds \tag{89}$$

Use

$$z_0(x) = \int_{x_1}^{x} I_\Delta(s)/I_\Sigma \, ds \tag{90}$$

as trial function for z. The beginning of the next step, (*iv*), is redundant, but is required for the iteration loop.

(*iv*) Set $E(x) = E_D(x) + (\epsilon v/I_\Sigma)z_0(x)$, and $I_\Delta = I_\Sigma z_0'$. Using these values, evaluate α, β, and H, (29).

(*v*) Solve

$$[D^2 + (\beta - \alpha)\, D - H]z = \alpha + \beta - Hz_0 \tag{91}$$

for z with boundary conditions $z' = -1$ at left boundary and $z = +1$ at right boundary.

(*vi*) Make z the new trial solution z_0.

(*vii*) Repeat steps (*iv*) through (*vi*) until z and z_0 differ negligibly. If the final field at x_1 differs appreciably from the trial field E_1 the boundaries are incorrectly defined, and steps (*i*) and following should be repeated with the current value $E(x_1)$ as trial field E_1. This time use $I_\Delta = z'I_\Sigma$ instead ot (84) and (85) as trial function for I in step (*ii*).

(*viii*) When the conditions of step (*vii*) are satisfied, i.e., when $z \approx z_0$ and $E(x_1) \approx E_1$, then E, $I_\Delta = z'I_\Sigma$, α, β, and H are the desired self-consistent dc quantities.

APPENDIX B

In this appendix we show how the complex resonance frequency $A = f_a + if_r$ at which the impedance goes to infinity can be obtained directly from (31), rather than by curve fitting of results obtained at a set of imaginary s-values $s = 0 + if$, or real frequencies. At resonance the normalized field z goes to infinity and therefore the right-hand side of (31) is negligible compared to the left-hand side, i.e., we have tbe homogeneous equation

$$[D^2 - k^2 + (\alpha + \beta)k + (\alpha - \beta)D - H]z = 0. \tag{92}$$

Solutions of (92) with boundary conditions (42) and (43) exist only for special values of k. The quantity $k(k - \alpha - \beta)$ may be considered the eigenvalue of (92). Of the possible k values we select the complex conjugate pair of smallest absolute value. Let k_0 be the k with positive imaginary part. Then

$$vk_0 = 2\pi(f_a + if_r) \tag{93}$$

is the desired resonance frequency.

Numerical values of k may be obtained as follows. The differential equation (92) is replaced by a set of appropriate difference equations for the values z_n of z at a set of meshpoints. This set of equations may be written in matrix form

$$M \cdot Z = 0, \tag{94}$$

where Z is a vector having the z_n for its elements. The matrix M, being derived from a second-order differential equation, is a "tridiagonal matrix", i.e., it has nonvanishing elements only on the main diagonal and the two adjacent diagonals. Now k must be chosen so that the determinant of M vanishes. If k_1 and k_2 are trial values and the corresponding values of the determinant are D_1 and D_2, then one may choose as next trial value

$$k_3 = -\frac{D_2(k_2 - k_1)}{D_2 - D_1} \tag{95}$$

and thus iteratively approach the desired value of k_0.

The frequency f_c of the zero is chosen so that F has the proper phase in the neighborhood of the resonance frequency. Let F be the current fraction at the complex frequency $s_1 = f_a + if_1$, where f_1 is near f_r, then

$$f_c = f_1 \frac{F_{\text{real}}}{F_{\text{imag}}} - f_a. \tag{96}$$

REFERENCES

1. Read, W. T., A Proposed High-Frequency Negative-Resistance Diode, B.S.T.J., *37*, March, 1958, pp. 401–466.
2. Johnston, R. L., DeLoach, B. C., Jr., and Cohen, B. G., A Silicon Diode Microwave Oscillator, B.S.T.J., *44*, February, 1965, pp. 369–372.
3. Lee, C. A., Batdorf, R. L., Wiegmann, W., and Kaminski, G., The Read Diode-An Avalanche Transit-Time, Negative Resistance Oscillator, Appl. Phys. Letters, March, 1965, pp. 89–91.
4. Misawa, T., private communication.
5. Josenhans, J. G., private communication.
6. Gilden, M. and Hines, M. E., Electronic Tuning Effects in the Read Microwave Avalanche Diode, IEEE Trans. on Electron Devices, January, 1966, pp. 169–175.
7. Josenhans, J. G. and Misawa, T., Experimental Characterization of a Negative Resistance Avalanche Diode, IEEE Trans. on Electron Devices, January, 1966, pp. 206–208.
8. Misawa, T., Negative Resistance in p-n Junctions Under Avalanche Breakdown Conditions, Parts I & II, IEEE Trans. on Electron Devices, January, 1966, pp. 137–151.
9. Scharfetter, D. L. and Gummel, H. K., Calculation of Large Signal Transients in Avalanche Diode Oscillators International Electron Devices Meeting, Washington, D. C., October 20–22, 1965, Paper 2.5.
10. Lee, C. A., Logan, R. A., Batdorf, R. L., Kleimack, J. J., and Wiegmann, W., Ionization Rates of Holes and Electrons in Silicon, Phys. Rev., *134*, May, 1964, pp. A761-A773.